J Opt (March 2023) 52(1):307–316
https://doi.org/10.1007/s12596-022-00876-2

RESEARCH ARTICLE

A new technique to optimize the properties of photonic crystal fibers supporting transmission of multiple orbital angular momentum modes

Haihao Fu[1] · Chao Liu[1] · Zao Yi[1,2] · Xinping Song[1] · Xianli Li[1] · Yanshu Zeng[1] · Jianxin Wang[1] · Jingwei Lv[1] · Lin Yang[1] · Paul K. Chu[3]

Received: 13 February 2022 / Accepted: 9 April 2022 / Published online: 9 May 2022

Abstract Spurred by the continuous development of orbital angular momentum (OAM) optical fiber communication technology, many photonic crystal fibers (PCFs) with excellent properties have been proposed. However, design and optimization of the performance of PCFs are usually complex. In this paper, a new optimization method is described and demonstrated on a LaSF09 high refractive index ring with a certain thickness inlaid in the central pore. The effective index difference, dispersion, effective mode area, nonlinear coefficient, numerical aperture (NA), OAM purity, walk-off length, and confinement loss at 1.55 μm are analyzed. A conventional photonic crystal fiber (PCF) that can transmit OAM modes is used to verify the method and our results reveal the validity and large potential of the method pertaining to the design and optimization of PCFs.

Keywords Orbital angular momentum · Photonic crystal fiber · Optical communication · Performance optimization

✉ Chao Liu
msm-liu@126.com

[1] School of Physics and Electronics Engineering, Northeast Petroleum University, Daqing 163318, People's Republic of China

[2] Joint Laboratory for Extreme Conditions Matter Properties, Southwest University of Science and Technology, Mianyang 621010, People's Republic of China

[3] Department of Physics, Department of Materials Science and Engineering, and Department of Biomedical Engineering, City University of Hong Kong, Tat Chee Avenue, Kowloon, Hong Kong, People's Republic of China

Introduction

On the heels of the continuous development of 5G, big data, and other network technologies, there is increasing demand for higher speed and better efficiency in communication [1]. The optical fiber communication technology has become a research hotspot in the field of communication because of the low cost, high confidentiality, and long-distance transmission [2]. In the classical electromagnetic field theory, the angular momentum of electromagnetic field is divided into spin angular momentum (SAM) related to circular polarization and orbital angular momentum (OAM) related to spatial helical phase structure. They always remain unchanged in the process of free space transmission. In 1992, Allen [3] pointed out that in a beam with helical phase factor $\exp(il\theta)$, each photon has OAM of $l\hbar$, where l is the azimuth index of the beam, also known as the topological charge, which reflects the number of times the optical vortex changes by 2π at a wavelength, and its size can be any integer from negative infinity to positive infinity. In addition, the generation methods of OAM mode can be divided into two categories. One is to output OAM mode directly from the laser cavity, and the other is to output Gaussian mode from the laser first, and then convert it to OAM mode. At present, the most commonly utilized OAM mode generation method is spiral phase slice method [4]. The incident light reflected by the helical phase plate will produce a beam with the corresponding OAM, and the conversion efficiency can reach 100% in theory. At the same time, since there are many orthogonal bases in the theories of OAM [5] and high-capacity mode division multiplexing (MDM) [6], there is a new degree of freedom about optical fiber communication. Similar to single-mode fibers (SMFs) [7] and few-mode fibers (MFMs) [8], many optical fibers can transmit OAM modes. Photonic crystal fibers (PCFs) [9–13] offer the capability of flexible

adjustment of the shape, size, number, position, and other parameters of air holes in the cladding to perform structural optimization. Therefore, they have become an excellent medium for transmission of OAM modes and different fiber structures have been proposed [14–18]. In 2012, Yang Yue [19] proposed a ring As_2S_3 PCF that can propagate 2 OAM modes, and the transmission of OAM modes in PCF has entered our vision. In 2018, Kecheng Zhang [18] designed a circular PCF which can support 110 OAM modes transmission in the range of 1.52–1.62 μm. Last year, Haihao Fu [20] realized the propagation of OAM modes in anti-resonant fiber for the first time.

However, the best properties cannot be easily obtained directly in the actual design of fibers and the dimensional parameters need to be optimized many times. In fact, most of the attempts are based on the experience of the designers but there have been few studies on the proper methodology to optimize the properties of optical fibers. Liu et al. [21] have proposed a photonic quasi-crystal fiber (PQF) supporting transmission of 10 OAM modes and the mode crosstalk is reduced based on the effects of the pore spacing on the effective index difference. Zhang et al. [22] have designed a PCF which can propagate 42 OAM modes and the influence of the radius of the central air hole on the confinement loss is studied. Ma et al. [23] have devised a high-capacity PCF boasting transmission of 180 OAM modes by adjusting the size of the central air hole. Although these methods can be used to optimize the properties of optical fibers to a certain extent, they have some disadvantages such as a single method, complex process, poor universal extension, and so on. Consequently, a better optimization method is crucial to OAM optical fiber communication.

Herein, by taking a common PCF that propagates OAM modes as an example, a very thin high-refractive index lanthanide optical glass ring (LaSF09) is inlaid in the central air hole. The finite element method (FEM) [24–27] is used to analyze the properties. The results show that compared with the non-inlaid fiber, the effective index difference, effective mode area, and OAM purity increase, but the dispersion, nonlinear coefficient, and confinement loss decrease. We also analyze the relationship between the ring thickness and effective index difference, dispersion, nonlinear coefficient, numerical aperture (NA), OAM purity, and confinement loss with the aid of the finite element software COMSOL. The optimization methodology demonstrated at 1.55 μm reveals large potential in the future development of PCFs for transmission of multiple OAM modes.

Fiber structure and basic theory

The OAM mainly exists in the vortex beam with a helical phase factor and is a natural attribute of light [28]. When the vortex light advances for a period, it can form a phase factor $exp(il\theta)$. At this time, its equal phase plane is 0 and the azimuth $\theta = 2\pi/l$. Since the vortex light can propagate infinitely many cycles, the number of phase angles is also infinite, so $\boldsymbol{l}$ can be any integer. In addition, because each $\boldsymbol{l}$ is an eigenstate that can carry free space quantum information, it can greatly increase the capacity of information transmission in communication, which has great potential in improving the capacity of optical communication system. [29]. Loading data information into the OAM beam provides a new means for information multiplexing. The pattern in the fiber is a representation of the spatial electromagnetic field distribution and the eigenvector modes can be obtained by solving the optical fiber with Maxwell equations. There are four eigenvector modes, namely TE, TM, HE, and EH, in the circular symmetrical optical fiber waveguide and the OAM modes can be defined as a series of eigenmodes with the same propagation constant [30]. These eigenmodes can be superimposed by the odd and even components of the corresponding HE mode or EH modes. The specific stacking method is shown in Eq. (1) [31]:

$$\begin{aligned} \mathbf{OAM}^{\pm}_{\pm l,m} &= \mathbf{HE}^{\mathbf{even}}_{l+1,m} \pm \mathbf{iHE}^{\mathbf{odd}}_{l+1,m} \\ \text{and} \quad \mathbf{OAM}^{\mp}_{\pm l,m} &= \mathbf{EH}^{\mathbf{even}}_{l-1,m} \pm \mathbf{iEH}^{\mathbf{odd}}_{l-1,m} \end{aligned} \tag{1}$$

where $\boldsymbol{l}$ and $\boldsymbol{m}$ are the number of topological charge and radial order, respectively, "$\pm$" and "$\mp$" in the upper right corner of the OAM represent the direction of circular polarization, and "+" is the right-hand circle polarization and "−" is the left-hand one. When $\boldsymbol{l}=1$, the order of EH module is 0, $\mathrm{OAM}^{\mp}_{\pm l,m}$ will not be synthesized. According to Eq. (1), OAM mode will have the identical polarization direction and rotation direction, and there are only two channels available for transmitting signals, so it can only exist as two information states. When $\boldsymbol{l}\geq 2$, it can exist as 4 channels. Therefore, the number of OAM modes propagating in the PCF is $4(\boldsymbol{l}-1)+2$.

LaSF09 is a familiar optical glass which can be used to manufacture substrates and PCFs, and its refractive index and material dispersion are determined by formula (2) [32]:

$$n^2(\lambda) - 1 = \frac{2.00029547\lambda^2}{\lambda^2 - 0.0121426017} + \frac{0.298926886\lambda^2}{\lambda^2 - 0.0538736236} + \frac{1.80691843\lambda^2}{\lambda^2 - 156.530829} \tag{2}$$

where λ is the wavelength. It should be illustrated that most materials in [4] can be used for the manufacture of high refractive index rings. However, the refractive index of PBG series glass is low, which is not conducive to the modulation of incident light. Although SK series has high refractive index, it is expensive and requires high temperature in the manufacturing process. The preparation of LaSF09

is relatively simple: after adding C_2H_5OH, H_2O and HCL at room temperature, it is heated to 80 °C and then placed in a thick solution. The gel fibers are drawn at room temperature, and LaSF09 fibers can be obtained when heated to about 600–800 °C. The high refractive index ring of LaSF09 can be obtained by drilling in the fiber center with rotary sonic drilling machine [33]. The refractive index of LaSF09 at 1.55 μm is 1.8133, which shows a tremendous effective index difference with the cladding materials. The refractive index of the material in the range of 1–2 μm is 1.8246–1.8061, which is relatively stable compared with other high refractive index materials. In addition, the refractive index of LaSF09 can be accurately controlled through the fiber annealing process [34], which greatly reduces the influence of the material itself while optimizing the fiber performance. Consequently, it is the most suitable performance optimization material. A thin and high refractive index ring inlaid in the central air hole can modulate the light in the optical fiber. The refractive index of LaSF09 is much larger than that of the background material SiO_2, and the light always tends to enter the medium with higher refractive index based on total internal reflection. Therefore, LaSF09 will attract the photons propagated in ring area. The refractive index of the OAM modes and light field distribution in the circular region can be changed when the ring thickness is altered, then the dispersion, nonlinear coefficient, and so on are changed. When optimizing the performance of PCF that can transmit OAM mode, the way of adjusting structural parameters is often adopted. The best performance parameters are obtained by studying the effects of the thickness of the annular region, the shape, size, number and spacing of cladding air-holes on dispersion, nonlinear coefficient, and confinement loss. However, the reason why it is more complex is that there are not only many parameter combinations, but also the parameters will affect each other. It will consume a lot of resources in the design of structure, which is not practical enough. The technique of inlaying LaSF09 in the central pore only needs to reasonably adjust the thickness of the ring to obtain the best performance, which greatly increases the optimization efficiency and has strong practicability. As long as the thickness of the ring is reasonably set, the communication performance of PCF can be optimized. In order to assess the feasibility of this optimization method, the conventional structure shown in Fig. 1 is chosen in our study.

The fiber is composed of a central air hole, a high refractive index ring, and two layers of air holes in the cladding with different radii. $\boldsymbol{R_1}$ and $\boldsymbol{R_2}$ are the radii of the central air hole and outer radius of the annular area, respectively. The values of $\boldsymbol{R_1}$ and $\boldsymbol{R_2}$ are optimized in the range of 4–6 μm and 2–3 μm. When $\boldsymbol{R_1}$ = 5.5 μm and $\boldsymbol{R_2}$ = 8 μm, dispersion is the flattest and the OAM purity is high. The optical fiber shows the lowest confinement loss when $\boldsymbol{d_1}$ = 1.6 μm and $\boldsymbol{d_2}$ = 3.6 μm are the diameters of the two air holes in the cladding with a spacing $\boldsymbol{\Lambda}$ = 0.2 μm. Consequently, we set $\boldsymbol{R_1}$ = 5.5 μm, $\boldsymbol{R_2}$ = 8 μm, $\boldsymbol{d_1}$ = 1.6 μm, $\boldsymbol{d_2}$ = 3.6 μm, and $\boldsymbol{\Lambda}$ = 0.2 μm. The red area in Fig. 1 is the LaSF09 high refractive index ring inlaid in the central air hole with a thickness of $\boldsymbol{h}$ = 0.1 μm and the blue area is the cladding made of SiO_2 which refractive index can be obtained by Eq. (3) [35]:

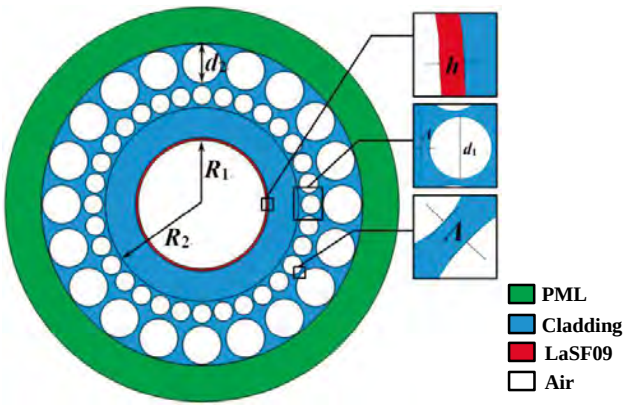

Fig. 1 Cross section of the PCF inlaid with the LaSF09 high refractive index ring

$$n^2(\lambda) = 1 + \frac{A_1\lambda^2}{\lambda^2 - B_1} + \frac{A_2\lambda^2}{\lambda^2 - B_2} + \frac{A_3\lambda^2}{\lambda^2 - B_3} \tag{3}$$

where $A_1 = 0.6961663$, $A_2 = 0.4079426$, $A_3 = 0.897479$, $B_1 = 0.0684043$, $B_2 = 0.1162414$, and $B_3 = 9.896161$. The green region is the perfect matching layer (PML) that can be regarded as an ideal absorber.

In actual fabrication, the sol–gel technique [36, 37] can be used to prepare the fiber. Before drawing the optical fiber, the LaSF09 ring needs to be made first. A circular hole can be drilled in the center of the cylindrical glass by using a rotary sonic drilling machine [33] to form a high refractive index ring. By using a catalyst, the materials are hydrolyzed and condensed to form the sol and then the gel is obtained after aging. At this time, the prepared LaSF09 high refractive index ring is combined in the center of the material by mechanical stamping or custom die extrusion given in [38], and the SiO_2 powder can be formed by the gel heat treatment and then made into the fiber preform, which is eventually pulled to form fibers by melt quenching. In a word, with the development of current industry, the technology of inlaying high refractive index glass ring into the center of the PCF can be realized in engineering.

Results and discussion

Compared with the conventional PCF that transmits OAM modes, embedding a high refractive index ring in the central pore can improve the properties of the fiber and the effects change with ring thickness. The second-order radial mode appears when the ring thickness is greater than 0.2 μm thus making demultiplexing difficult. Consequently, our study focuses on the impact of the ring thickness on the effective refractive index and effective index difference, dispersion, effective mode area and nonlinear coefficient, numerical aperture (NA), OAM purity, walk-off length and confinement loss in the range of 0–2 μm.

Transmitted modes

According to the theory, OAM modes are composed of the HE and EH modes which can be obtained by COMSOL simulation. Figures 2a–f show the light field distributions of the partial HE and EH modes that can be transmitted in the optical fiber in the z direction and Fig. 2g–i reveal the phase distributions corresponding to the OAM modes at 1.55 μm.

The light field distributions show that the energy of all the modes is limited to the annular region and only a little portion of the light leaks into the cladding. At the same time, the light field of the HE mode is closer to the cladding but that of the EH mode is closer to the core. This is the typical method to distinguish HE and EH modes. The red and blue regions in the figure not only represent the magnitude of the mode electric field intensity, but also show the number of the topological charges of different modes. In the OAM modes transmitted in this structure, the maximum number of topological charges is 5. Therefore, according to Eq. (1), the number of the OAM modes that can be transmitted in the PCF is $4\times5+2=22$, including $\mathrm{OAM}^{\pm}_{\pm 1,1}\{\mathrm{HE}_{2,1}\}$ and $\mathrm{OAM}^{\pm}_{\pm l,1}\{\mathrm{HE}_{l+1,1}, \mathrm{EH}_{l-1,1}\}$ ($l=1$–5). Moreover, the phase distributions of the OAM modes change in azimuth $\pi/2$. The vortex beam rotates around the optical axis once and the phase variable is $2n\pi$ when the topological charge $\boldsymbol{l}$ is $\boldsymbol{n}$, which can be demultiplexed by the conjugate phase mode.

Effective refractive index

The effective refractive index which can determine the effective index difference and dispersion is a basic physical quantity in OAM optical fiber communication. Moreover, the refractive index can also affect the performance of the optical device [39, 40]. The effective refractive index of OAM modes can be transformed by inlaying a high refractive index ring with a certain thickness in the central air hole of the PCF. The variation of ring thickness with effective refractive index is shown in Fig. 3.

With increasing ring thickness, the effective refractive indexes of the HE and EH modes increase because the speed of light decreases when the beam enters LaSF09. When the ring thickness is less than 0.125 μm, because the photon numbers of the HE and EH modes close to the core are almost the same and the influence of the high refractive index ring on them is also the same, the refractive index increases to the same extent. When the ring thickness is greater than 0.125 μm, the reason why the EH mode is greatly affected is that the EH mode is closer to the core. The rate of refractive index increase becomes smaller but the HE mode is not influenced as much. Therefore, the effective

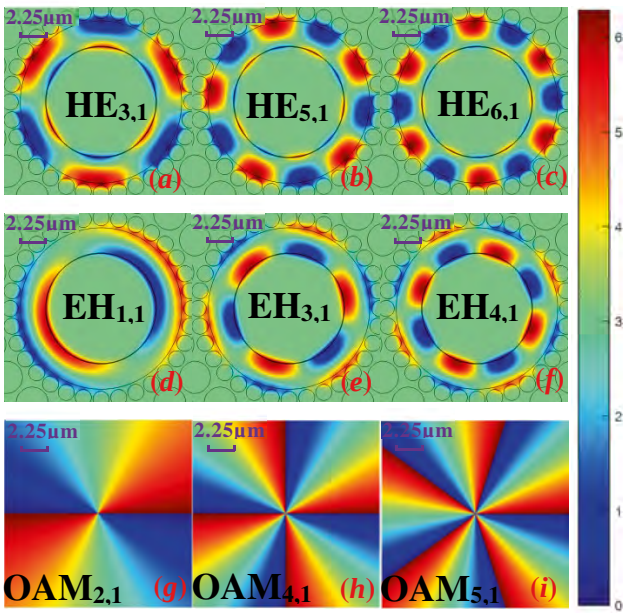

Fig. 2 **a–f** Optical field distributions of the partial HE and EH modes in the z direction and **g–i** Phase diagrams of some displayed OAM modes

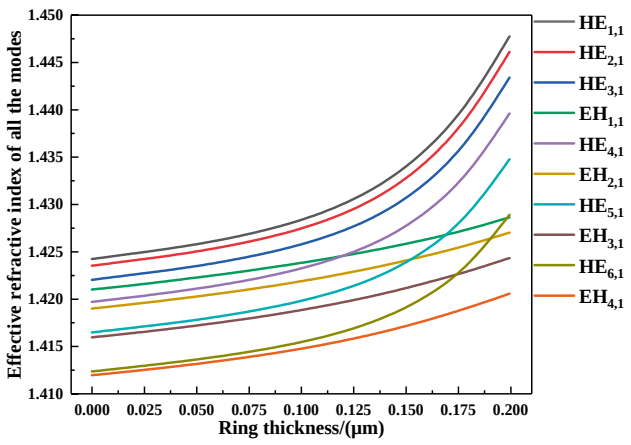

Fig. 3 Relationship between the effective refractive index and ring thickness

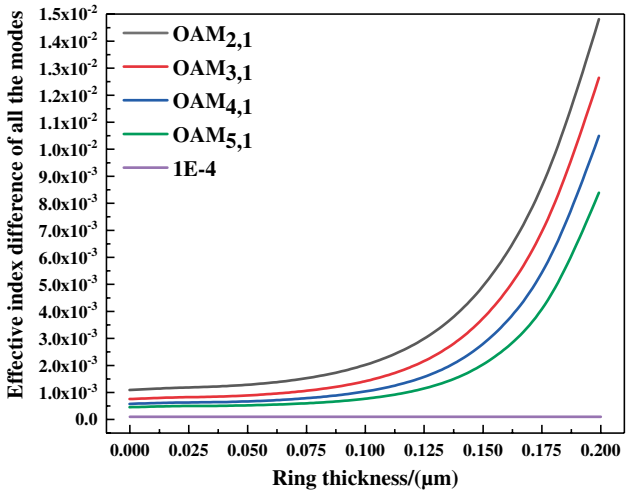

Fig. 4 Effective index difference of the OAM modes directly proportional to the ring thickness

refractive index of the HE modes increases faster than that of the EH modes at 1.55 μm.

The basic requirement of OAM modes transmission in PCFs is that the effective index difference between the HE and EH modes which synthesize the same order OAM is greater than 1×10^{-4} [41], otherwise the OAM modes will degenerate into the linear polarization (LP) modes resulting in large inter-mode crosstalk. Figure 4 shows that the effective index difference of all OAM modes is greater than 1×10^{-4} and directly proportional to the thickness of the ring. When the ring thickness is bigger than 0.125 μm, the increasing rate of the effective index difference becomes larger, which is conducive to stable propagation of OAM modes at 1.55 μm.

Chromatic dispersion

Dispersion is the phenomenon of pulse broadening caused by different mode components of optical signals transmitted at different speeds over a certain distance in optical fibers. Because pulse broadening produces signal distortion and debases the efficiency of optical communication, dispersion must be controlled when designing and optimizing optical fibers. Dispersion in optical fibers is mainly composed of materials dispersion and waveguide dispersion. Materials dispersion of SiO_2 and LaSF09 depends on the materials properties determined by Eqs. (2) and (3) and waveguide dispersion is mainly decided by the effective refractive index of the OAM modes. Consequently, the total dispersion can be obtained by Eq. (4) [42]:

$$D = D_{\mathrm{m}}(\lambda) + D_{\mathrm{w}}(\lambda) = -\frac{\lambda}{c}\frac{d^2\mathrm{Re}\left(n_{\mathrm{eff}}\right)}{d\lambda^2} \tag{4}$$

where $D_{\mathrm{m}}(\lambda)$ and $D_{\mathrm{w}}(\lambda)$ are the materials and waveguide dispersion, respectively, λ is the wavelength, $c=3\times10^8$ m/s is the speed of light, and $\mathrm{Re}(n_{\mathrm{eff}})$ is the real part of effective refractive index. The beam velocity changes when light enters the high refractive index ring inlaid in the central pore affecting dispersion. By adjusting the thickness of the ring, dispersion can be optimized and the relationship between the ring thickness and dispersion is illustrated in Fig. 5.

After inlaying a thin high-refractive index ring, dispersion of all the OAM modes decreases resulting in better efficiency in optical communication. With increasing effective refractive index, the speed of light propagating in the fiber decreases and dispersion diminishes. When the ring thickness is larger than 0.125 μm, negative dispersion arises due to the large change in the refractive index of the HE modes. As for the EH modes, owing to the small change in the refractive index, dispersion continues to decrease, but there is no negative dispersion.

Effective mode area and nonlinear coefficient

The effective mode area refers to the domain of the mode field distribution area, which reflects the concentration of photon energy. A large effective mode area not only increases the energy storage and pulse energy of the optical fiber, but also increases the absorption efficiency of the optical fiber to light source. The effective mode area can be computed by Eq. (5) [43]:

$$A_{\mathrm{eff}} = \frac{\left(\iint |E(x,y)|^2 dxdy\right)^2}{\iint |E(x,y)|^4 dxdy} \tag{5}$$

where $E(x, y)$ is the light field distribution and the numerator and denominator in the formula can be obtained by COMSOL simulation. The nonlinear effect refers to that caused by nonlinear polarization of the medium under the

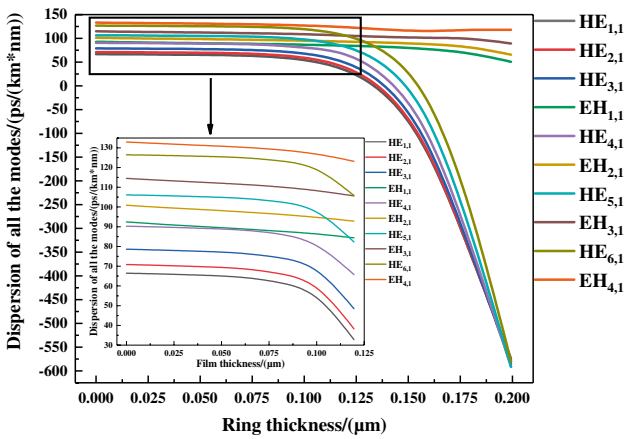

Fig. 5 Relationship between dispersion and ring thickness

action of strong light. The nonlinear coefficient is a physical quantity to determine the nonlinear effect, which is inversely proportional to the effective mode area and derived by Eq. (6) [44]:

$$\gamma = \frac{2\pi n_2}{\lambda A_{\text{eff}}} \tag{6}$$

where λ is the wavelength, A_{eff} is the effective mode area, and $n_2 = 2.3 \times 10^{-20}$ m^2/W [45] is the nonlinear refractive index coefficient of SiO_2. It should be paid attention that the research object is the OAM modes transmitted in the annular region when calculating the nonlinear coefficient, and the variation of the nonlinear coefficient of OAM modes after inlaying the high refractive index ring is mainly studied. In addition, compared with the circular region, the thickness of the LaSF09 ring is very small. Therefore, the influence of LaSF09 itself is not considered. When a high refractive index ring is embedded in the central air hole, the effective mode area changes and Fig. 6a and b reveal the changes in the effective mode area, nonlinear coefficient, and ring thickness at 1.55 μm.

After inlaying a very thin high refractive index ring, the light field diffuses into the ring. The effective mode area increases and the nonlinear coefficient decreases. When the ring thickness is greater than 0.075 μm and less than 0.125 μm, the effective mode area decreases slightly. When the ring thickness is bigger than 0.125 μm, because the refractive index of LaSF09 is much greater than SiO_2 and light tends to propagate in the medium with a bigger refractive index, the light fields of the HE and EH modes are focused in the core. Hence, the effective mode area and nonlinear coefficient decrease and increase, respectively. Diminution of the effective mode area of the EH modes abates less than that of the HE modes because the EH modes are more stable. Consequently, the method of embedding a high refractive index ring and controlling the thickness can determine the maximum effective mode area and minimum nonlinear coefficient when optimizing the optical fiber.

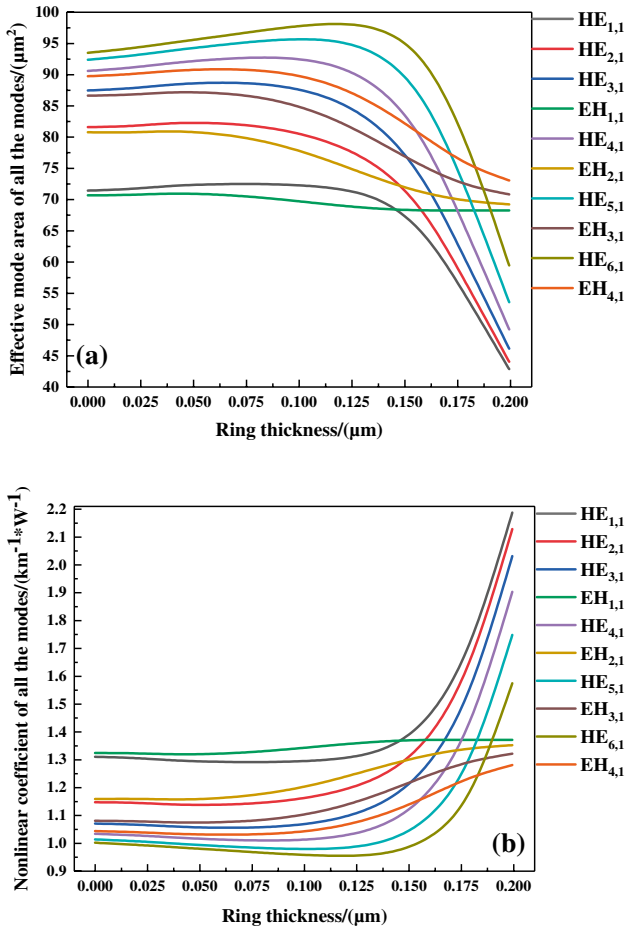

Fig. 6 **a** and **b** Variations of the effective mode area, nonlinear coefficient, and ring thickness at 1.55 μm

Numerical aperture

The numerical aperture (NA) of the optical system is a dimensionless constant used to measure the angle range of light that can be collected by the system and reflects the coupling efficiency between the optical fiber and light source. The entity can be calculated by Eq. (7) [46]:

$$\text{NA} = \left(1 + \frac{\pi A_{\text{eff}}}{\lambda^2}\right)^{\left(-\frac{1}{2}\right)} \tag{7}$$

where λ is the wavelength and A_{eff} is the effective mode area determined by Eq. 5. The larger the NA, the stronger is the coupling efficiency between the fiber and illuminant. Figure 7 shows the effects of altering the ring thickness on NA at 1.55 μm.

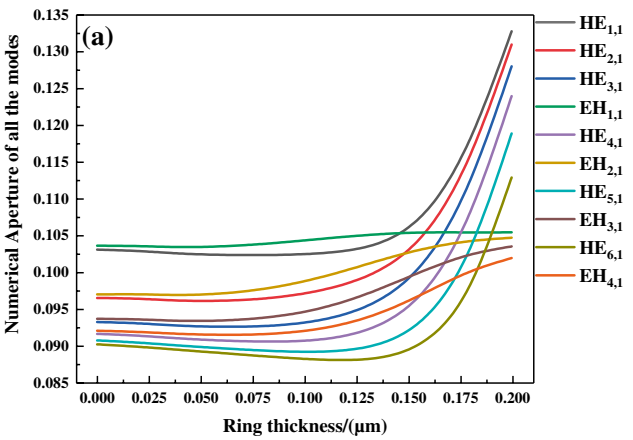

Fig. 7 Effects of ring thickness on NA at 1.55 μm

The NA of the HE and EH modes goes up with ring thickness when the ring thickness is small but changes a little otherwise. The NA of the HE modes increases when the thickness of the ring is greater than 0.125 μm because the optical field converges to the core to reduce the effective mode area. In conclusion, inlaying a high refractive index ring in the central pore is instrumental to improving the NA of the OAM modes.

OAM purity

The OAM purity can be defined as the ratio of the core field strength to the overall cross-sectional field strength. The higher the purity of the OAM modes, the more stable is optical fiber communication. A high OAM purity can also reduce the confinement loss and increase the propagation distance. The OAM purity can be obtained by Eq. (8) [22]:

$$\eta = \frac{I_r}{I_c} = \frac{\iint_{\text{ring}} |\overrightarrow{E}|^2 dxdy}{\iint_{\text{cross - section}} |\overrightarrow{E}|^2 dxdy} \tag{8}$$

where I_r and I_c are the field intensity of the circular area and hole cross-section of the fiber, respectively, which can be obtained with COMSOL. Inlaying a high refractive index ring changes the light field distribution in the optical fiber and varies the OAM purity. The relationship between the OAM purity and ring thickness at 1.55 μm is displayed in Fig. 8.

When the ring thickness is less than 0.02 μm, light enters the high refractive index ring from the annular region and the OAM purity decreases. The reason for the increase of OAM purity is that light tends to enter the medium with a high refractive index and light leaks into the cladding entering the annular region. The light capacity of the high refractive index ring increases when the ring thickness is bigger than 0.125 μm. The number of photons in the ring region decreases and the purity of OAM decreases. Since the EH modes are closer to the core and more stable, the variation in the purity is not large relative to the HE modes. Besides, although the OAM purity decreases after inlaying the LaSF09 on the inner wall of the central pore, the mode purity only dwindles 0.23% approximately compared with the non-inlaid when the ring thickness is 0.125 μm, and it is acceptable. However, the mosaic of LaSF09 has conspicuously improved other performances, so the technique is still of great significance to enlarge the communication efficiency of optical fiber.

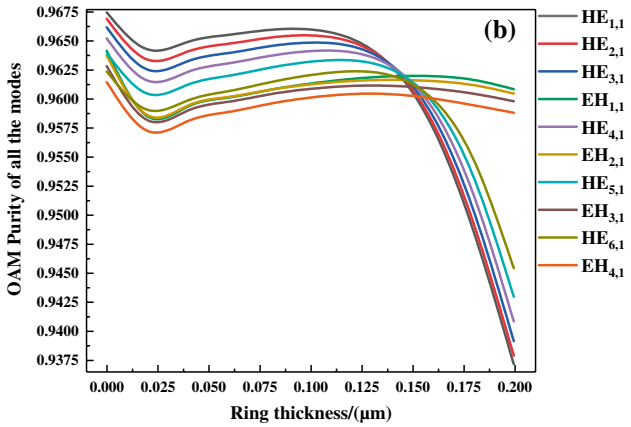

Fig. 8 Relationship between the OAM purity and ring thickness at 1.55 μm

Walk-off length and confinement loss

The transmission distance of OAM modes in the PCF must be considered when designing and optimizing optical fibers. The propagation distance of OAM modes is mainly related to the walk-off length and confinement loss of the modes. Odd and even modes have walk-off effects because they have different transmission rates in optical fibers. When the OAM mode is transmitted in the optical fiber, if the walk-off effect is too large, the odd and even modes no longer synthesize OAM modes. The 10 ps walk-off length is a physical quantity used to analyze the walk-off effect, which is defined as [47]:

$$L_{10\text{ps}} = \frac{c \times 10\text{ps}}{n_{\text{eff}}^{\text{even}} - n_{\text{eff}}^{\text{odd}}} = \frac{3 \times 10^{-3}}{n_{\text{eff}}^{\text{even}} - n_{\text{eff}}^{\text{odd}}}(m) \tag{9}$$

where c is the speed of light and n_{eff}^{even}, n_{eff}^{odd} are the effective refractive indexes of the even and odd modes, respectively. Since different air holes in the PCF have different limiting ability to light wave, the loss caused by partial energy leakage to the cladding is the confinement loss which is inversely proportional to the distance of OAM modes transmitted in the PCF as shown in Eq. (10) [23, 48]:

$$L = \frac{2\pi}{\lambda} \frac{20}{\ln(10)} 10^6 \text{Im}(n_{\text{eff}}) \tag{10}$$

where λ is the wavelength and $\text{Im}(n_{\text{eff}})$ is the imaginary part of the effective refractive index. Figures 9a and b exhibit the variations of the 10 ps walk-off length and confinement loss with ring thickness at 1.55 μm, respectively.

Compared to the PCF without the inlaid high refractive index ring, the walk-off length of all OAM modes increases by hundreds of times, thereby conducive to long-distance transmission of the OAM modes. When the ring thickness is larger than 0.10 μm, the walk-off length begins to decrease. Consequently, embedding a high refractive index ring not only improves the walk-off length and enhances the transmission distance of OAM modes in the PCF, but also attains the maximum walk-off length through the thickness

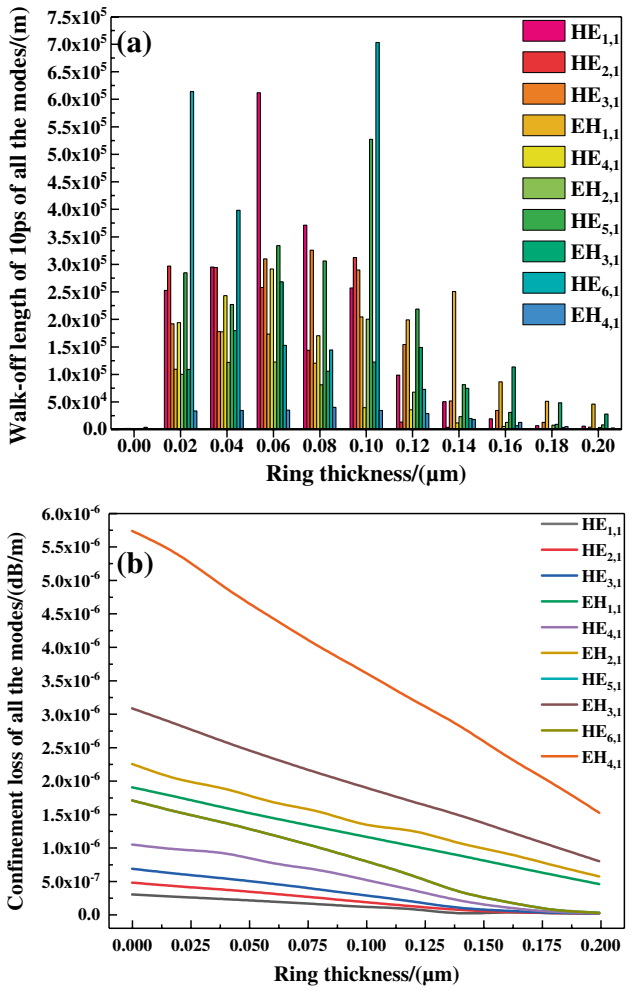

Fig. 9 Variation of the 10 ps walk-off length and confinement loss with ring thickness at 1.55 μm

of modulation ring, which is of great value in the design and optimization of PCFs. In addition, the larger confinement loss of high-order modes is attributed to that the limiting ability of the ring region to the high-order modes is lower, and the EH mode confinement loss is higher at the same wavelength compared with HE mode. Figure 9b indicates that inlaying with LaSF09 high refractive index ring can effectively reduce the confinement loss of all OAM modes, especially high-order modes. Moreover, the ring thickness is inversely proportional to the confinement loss, and the confinement loss in long-distance and stable transmission can be reduced by hundreds of times for thicker ring.

The analysis of usefulness

From the results of numerical simulation, inlaying a certain thickness of LaSF09 high refractive index ring in the central pore of PCF has greatly improved the performance of OAM mode, which is an effective performance optimization method, and it has great application and potential in reasonably designing the structure of PCF to make it have higher communication efficiency. Moreover, mechanical stamping or custom die extrusion can embed high refractive index into the central pore, and the current technology is completely feasible. In addition, the traditional method of adjusting the thickness of annular area and the arrangement of cladding air holes is usually adopted when optimizing the performance of OAM modes transmitted in PCF. This method involves many variables and will bring a lot of trouble in optimization. The method of inlaying high refractive index ring only needs to consider the variable of ring thickness, which is more novel and practical.

Conclusion

A novel method is described to optimize the performance of PCFs for transmission of multiple OAM modes. A thin LaSF09 high refractive index ring is inlaid in the central pore and the method is also assessed using a conventional PCF structure at 1.55 μm. Numerical analysis of the ring thickness in the range of 0.00 to 2.00 μm indicates that by varying the thickness of the high refractive index ring, the effective index difference, dispersion, walk-off length, and confinement loss can be optimized to determine the best parameters. The methodology and results reveal the potential in designing and optimizing PCFs for transmission of multiple OAM modes.

Funding The work was jointly supported by Postdoctoral Scientific Research Development Fund of Heilongjiang Province [LBH-Q20081], Local Universities Reformation and Development Personnel Training Supporting Project from Central Authorities [140119001], and City University of Hong Kong Strategic Research Grant (SRG) [Grant Number 7005505] and Science and Technology Planning Project of Guangdong Province [2018A01006].

Declarations

Conflict of interest The authors declare no conflicts of interest.

References

1. D.J. Richardson, J.M. Fini, Space-division multiplexing in optical fibres. Nat. Photonics **7**, 354–362 (2013)
2. R. Ryf, S. Randel, A.H. Gnauck et al., Space-division multiplexing over 10 km of three-mode fiber using coherent 6x6 MIMO processing. J. Lightwave Technol. **30**, 521–531 (2011)
3. L. Allen, M.W. Beijersbergen, R.J.C. Spreeuw et al., Orbital angular momentum of light and the transformation of Laguerre-Gaussian laser modes. Phys. Rev. A **45**(11), 8185 (1992)
4. V.V. Kotlyar, A.A. Almazov, S.N. Khonina et al., Generation of phase singularity through diffracting a plane or Gaussian beam by a spiral phase plate. JOSA A **22**(5), 849–861 (2005)

5. F. Parmigiani, Y. Jung, L. Grünernielsen, et al, MIMO-less space division multiplexing transmission over 1 km elliptical core few mode fiber. Cleo, (2017)
6. N. Bozinovic, Y. Yue, Y. Ren et al., Terabit-scale orbital angular momentum mode division multiplexing in fibers. Science **340**, 1545–1548 (2013)
7. A. Vigneswaran, Mahendran, Study on 20 and 50 Gbps soliton transmission in conventional single mode fiber (SMF). IEEE, (2014)
8. F. Yaman, N. Bai, B. Zhu et al., Long distance transmission in few-mode fibers. Opt. Express **18**, 132–507 (2010)
9. E. Liu, S. Liang, J. Liu, Double-cladding structure dependence of guiding characteristics in six-fold symmetric photonic quasi-crystal fiber. Superlattices Microstruct. **130**, 61–67 (2019)
10. W. Liu, Y. Shi, Z. Yi, C. Liu, F. Wang, X. Li, J. Lv, L. Yang, P.K. Chu, Surface plasmon resonance chemical sensor composed of a microstructured optical fiber for the detection of an ultra-wide refractive index range and gas-liquid pollutants. Opt. Express **29**, 40734–40747 (2021)
11. C. Li, B. Yan, J. Liu, Refractive index sensing characteristics in a D-shaped photonic quasi-crystal fiber sensor based on surface plasmon resonance. J. Opt. Soc. Am. A **36**, 1663–1668 (2019)
12. E. Liu, W. Tan, B. Yan, J. Xie, R. Ge, J. Liu, Broadband ultra-flattened dispersion, ultra-low confinement loss and large effective mode area in an octagonal photonic quasi-crystal fiber. J. Opt. Soc. Am. A **35**, 431–436 (2018)
13. B. Yan, A. Wang, E. Liu, W. Tan, J. Xie, R. Ge, J. Liu, Polarization filtering in the visible wavelength range using surface plasmon resonance and a sunflower-type photonic quasi-crystal fiber. J. Phys. D Appl. Phys. **51**, 155105 (2018)
14. Y. Yue, Z. Lin, Y. Yan et al., Octave-spanning supercontinuum generation of vortices in an As_2S_3 ring photonic crystal fiber. Opt. Lett. **37**, 1889–1891 (2012)
15. L. Xi, W. Tian, X. Zhang, A circular photonic crystal fiber supporting 26 OAM modes. Opt. Fiber Technol. **30**, 184–189 (2016)
16. X. Bai, H. Chen, Y. Zhuang et al., A new type Bragg fiber for supporting 50 orbital angular momentum modes. Optik **219**, 165153 (2020)
17. L. Yu, X. Xun, W. Ning et al., Numerical analysis of a photonic crystal fiber for supporting 76 orbital angular momentum modes. J. Opt. **20**(10), 105701 (2018)
18. L. Zhang, K. Zhang, J. Peng et al., Circular photonic crystal fiber supporting 110 OAM modes. Opt. Commun. **429**, 189–193 (2018)
19. Y. Yue, L. Zhang, Y. Yan et al., Octave-spanning supercontinuum generation of vortices in an As_2S_3 ring photonic crystal fiber. Opt. Lett. **37**(11), 1889–1891 (2012)
20. H. Fu, Z. Yi, Y. Shi et al., Circular anti-resonance fibre supporting orbital angular momentum modes with flat dispersion, high purity and low confinement loss. J. Mod. Opt. **68**(15), 784–791 (2021)
21. E. Liu, W. Tan, B. Yan et al., Robust transmission of orbital angular momentum mode based on a dual-cladding photonic quasi-crystal fiber. J. Phys. D Appl. Phys. **52**, 325110 (2019)
22. H. Zhang, X. Zhang, H. Li et al., A design strategy of the circular photonic crystal fiber supporting good quality orbital angular momentum mode transmission. Opt. Commun. **397**, 59–66 (2017)
23. Q. Ma, A.P. Luo, W. Hong, Numerical study of photonic crystal fiber supporting 180 orbital angular momentum modes with high mode quality and flat dispersion. J. Lightwave Technol. **39**, 2971–2978 (2021)
24. J.N. Reddy, *An introduction to the finite element method* (John Wiley & Sons, Ltd, 2013)
25. Y. Deng, G. Cao, Y. Wu et al., Theoretical description of dynamic transmission characteristics in MDM waveguide aperture-side-coupled with ring cavity. Plasmonics **10**, 1537–1543 (2015)
26. G. Cao, H. Li, D. Yan et al., Systematic theoretical analysis of selective-mode plasmonic filter based on aperture-side-coupled slot cavity. Plasmonics **9**, 1163–1169 (2014)
27. F. Zhou, F. Qin, Z. Yi et al., Ultra-wideband and wide-angle perfect solar energy absorber based on Ti nanorings surface plasmon resonance. Phys. Chem. Chem. Phys. **23**, 17041–17048 (2021)
28. A.M. Blackburn, J.C. Loudon, Vortex beam production and contrast enhancement from a magnetic spiral phase plate. Ultramicroscopy **136**, 127–143 (2014)
29. L. Allen, M.W. Beijersbergen, R. Spreeuw et al., Orbital angular momentum of light and transformation of Laguerre Gaussian Laser modes. Phys. Rev. A **45**, 8185–8189 (1992)
30. C. Brunet, P. Vaity, Y. Messaddeq et al., Design, fabrication and validation of an OAM fiber supporting 36 states. Opt. Express **22**, 26117–16127 (2014)
31. T. He, B. Wu, Low confinement loss photonic crystal fibre capable of supporting 54 orbital angular momentum modes. J. Mod. Opt. **67**, 1–7 (2020)
32. F. Wang, C. Liu, Z. Sun et al., A highly sensitive SPR sensors based on two parallel PCFs for low refractive index detection. IEEE Photonics J. **10**(4), 1–10 (2018)
33. X. Feng, A.K. Mairaj, D.W. Hewak et al., Nonsilica glasses for holey fibers. J. Lightwave Technol. **23**(6), 2046 (2005)
34. J. Hsu, Liao, Diode-laser-pumped glass-clad Ti: sapphire crystal-fiber-based broadband light source. IEEE Photonics Technol. Lett. **24**, 854–856 (2012)
35. C. Liu, J. Lü, W. Liu, F. Wang, P.K. Chu, Overview of refractive index sensors comprising photonic crystal fibers based on the surface plasmon resonance effect [Invited]. Chin. Opt. Lett. **19**(10), 102202 (2021)
36. M. Ahabboud, T. Lamcharfi, F. Abdi et al., Effect of Cu doping on structural and dielectric properties of Pb1-xCux(Zr0.52Ti0.48) O3(PCxZT) ($0 \leq x \leq 0.2$) ceramics prepared by sol-gel method. Asian J. Chem. **33**, 665–670 (2021)
37. V.V.R.K. Kumar, A.K. George, W.H. Reeves et al., Extruded soft glass photonic crystal fiber for ultrabroad supercontinuum generation. Opt. Express **10**(25), 1520–1525 (2002)
38. V. Matejec, M. Hayer, J. Mrazek et al., Performance of the sol-gel method for the preparation of optical fibers. Rev. Roum. Chim. **52**, 991 (2007)
39. W. Xianglong, Y. Zheng, Y. Luo, J. Zhang, Z. Yi, Wu. Xianwen, S. Cheng, W. Yang, Y. Yang, W. Pinghui, Phys. Chem. Chem. Phys **23**(47), 26864–26873 (2021)
40. Y. Deng, G. Cao et al., Dynamic control of double plasmon-induced transparencies in aperture-coupled waveguide-cavity system. Plasmonics **13**, 345–352 (2018)
41. M.A. Kabir, M.M. Hassan, K. Ahmed et al., Novel spider web photonic crystal fiber for robust mode transmission applications with supporting orbital angular momentum transmission property. Opt. Quantum Electron. (2020). https://doi.org/10.1007/s11082-020-02447-w
42. X. Bai, Chen et al., Design of a circular photonic crystal fiber with square air-holes for orbital angular momentum modes transmission. Optik **158**, 1266–1274 (2018)
43. S.H. Huang et al., Microstructure ring fiber for supporting higher-order orbital angular momentum modes with flattened dispersion in broad waveband. Appl. Phys. B **125**(11), 1–8 (2019)
44. Z. Hu, W. Zhang, L. Xi et al., A new type circular photonic crystal fiber for orbital angular momentum mode transmission. IEEE Photonics Technol. Lett. **28**, 1426–1429 (2016)
45. X. Wan, Z. Wang, B. Sun et al., Low dispersion and confinement loss photonic crystal fiber for orbital angular momentum mode transmission. Opt. Quantum Electron. **52**, 6 (2020)
46. S.M. Islam, J. Sultana et al., A novel approach for spectroscopic chemical identification using photonic crystal fiber in the terahertz regime. IEEE Sens. J. **18**, 575–582 (2018)

47. Y. Yue, Y. Yan, N. Ahmed et al., Mode and propagation effects of optical orbital angular momentum (OAM) modes in a ring fiber. Optical Society of America (2012)
48. S. An, J. Lv, Z. Yi et al., Ultra-short and dual-core photonic crystal fiber polarization splitter composed of metal and gallium arsenide. Optik **226**, 165779 (2021)